Optics Communications 290 (2013) 87–91

Contents lists available at SciVerse ScienceDirect

Optics Communications

journal homepage: www.elsevier.com/locate/optcom

Discussion

Slow light property in ring-shape-hole slotted photonic crystal waveguide

Kong-Tao Zhu, Tian-Song Deng, Yan Sun, Qi-Feng Zhang, Jin-Lei Wu *

Key Laboratory for the Physics and Chemistry of Nanodevices, Department of Electronics, Peking University, Beijing 100871, People's Republic of China

ARTICLE INFO

Article history:
Received 20 June 2012
Received in revised form
17 October 2012
Accepted 17 October 2012
Available online 7 November 2012

Keywords:
Slow light
Ring-shape-hole
Photonic crystal
Waveguide

ABSTRACT

Slow light in photonic crystal waveguide is now being heavily investigated for applications in optical devices. A ring-shape-hole slotted PhCW (RSPhCW) is designed in the paper. Band structures and group indices are calculated through plane wave expansion method. Flat band slow light property is observed, which provides low group velocity dispersion and avoids high speed optics signal from distortion in transmission. A method is proposed by tuning the positions of the first and second rows with the ring-shape-holes adjacent to the slot, which can tune the group index and the bandwidth of the guided band at the same time. This method is used to optimize the slow light property of the RSPhCW. The bandwidths ranging from 1.8 nm to 17.3 nm for group indices from 15 to 67 are obtained. From the point of view of reality, this method has its advantage of fabricating than tuning the outer and inner radii of the ring-shape-holes.

© 2012 Elsevier B.V. All rights reserved.

1. Introduction

Slow light in photonic crystal waveguide (PhCW) has attracted a great deal of attention for its wide applications in optical devices [1–6]. Extensive PhCW structures have been proposed to realize slow light both in theory and experiment [7–12]. Conventional PhCWs are usually constructed on slabs with triangular lattice of air holes. Although slow light properties in conventional PhCWs with flat bands and low group velocities have been realized [13–15], light in conventional PhCWs is usually seriously confined in the high index guiding layer, which may disturb the interaction between light and low index materials.

Slotted PhCWs (SPhCWs) were first presented by Almeida et al. [16], which can confine light in void nanostructure, namely, a narrow slot filled with low-index materials. The properties of the efficient interaction between light and materials and the high confinement of light to a nanometer-sized region make this structure an attractive technology in optical sensing devices [17], optical probes [18], all-optical switching [19], et al. Slow light with group index of 150 is also realized in such a structure [20]. However, slow light modes, which have low group velocity accompanied with large group velocity dispersion (GVD), would distort the pulse shape and cause severe degradation in high speed optics signal transmission [21]. Therefore low GVD is very important to maintain the transmission signal stable and undistorted in slow light devices.

Though recent studies have revealed excellent slow light properties, there are still some drawbacks. Refs. [13–15] are about conventional PhCWs, in which the waveguide core is constructed with high-index materials. Thus the light is highly confined in the high-index materials. The interaction between light and low-index materials will be counteracted. Refs. [17,20] are slotted PhCWs and the flat band is missed. The group index is as high as 150, but the bandwidth is very narrow and the GVD values are not low, which will induce a severe degradation in the light transmission.

Slow light with a wide bandwidth is also very useful. The normalized delay-bandwidth product (NDBP) is considered as an essential criterion for slow light optical device properties. Ring-shape-hole photonic crystals waveguides (RPhCWs) have been theoretically demonstrated for its flat band slow light property and large NDBP values [22]. Theoretical results show that both the outer and inner radii of the ring-shape-holes in the first and second row adjacent to the waveguide core affect the slow light properties [23–26].

To get both the advantages of SPhCWs and RPhCWs, a new PhCW is designed. In this paper, we study the slow light property of a RSPhCW. Considering the available technique in experiments, the positions of the first and second ring-shape-holes adjacent to the slot are chosen as the tuning parameters. They are used to optimize the slow light property of the PhCW. The effects of these parameters on the group index n_g, namely, the reciprocal of the group velocity v_g are discussed systematically. Finally, the optimized examples of the RSPhCW with high group indices and low GVD values are given.

2. Design and modeling

The basic structure is a triangular lattice photonic crystal (PhC) slab consisting of circular air holes (radii $r=0.34a$) with lattice

* Corresponding author. Tel./fax: +86-10-62761333.
E-mail address: jlwu@pku.edu.cn (J.-L. Wu).

0030-4018/$ - see front matter © 2012 Elsevier B.V. All rights reserved.
http://dx.doi.org/10.1016/j.optcom.2012.10.055

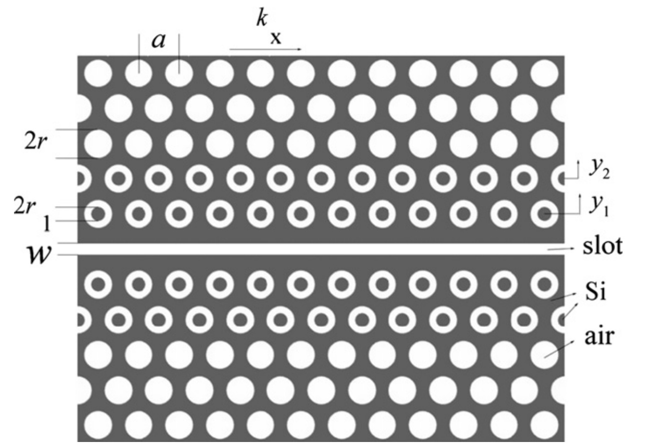

Fig. 1. Schematic structure of the RSPhCW. Radii $r=0.34a$, $r_1=0.17a$. k_x represents the wave vector. The arrows of y_1, y_2 represent the positive direction, respectively. Black denotes silicon and white denotes air. Here, $w=0.28a$, $y_1=0a$, $y_2=0a$.

constant a ($a=520$ nm to set the central wavelength at 1550 nm) in a dielectric silicon background ($\varepsilon=11.56$). As shown in Fig. 1, the central line of air holes is replaced with a narrow air slot with the width w. Additional dielectric pillars (radii $r_1=0.17a$, $\varepsilon=11.56$) are added to the first and second line of air holes adjacent to the slot. Two-dimensional (2D) plane wave expansion method (PWEM) is employed with the effective slab index of 2.9 for the 210 nm thick slab in our model. The supercell method is used in the calculation [8,27]. The supercell size is set to $a\times 11a$, which is large enough that the coupling between the adjacent parallel waveguides can be neglected.

The dispersion curves for TE polarized light-wave are calculated, in which the direction of the electric field is in parallel with the holes. The MIT photonic-band package is used, which is software adopting the PWEM, to simulate the band frequency of the RSPhCW.

The group velocity v_g of the guided modes equals the slope of the dispersion curve.

$$v_g=\frac{d\omega}{dk}=\frac{c}{n_g} \tag{1}$$

here, ω is the frequency, k is the wave vector in the propagation direction (it is k_x in Fig. 1), c is the velocity of light in vacuum, n_g is the group index. From this formula, n_g can be expressed as

$$n_g=c\frac{dk}{d\omega} \tag{2}$$

The GVD value β_2 is given by the second order derivative of the dispersion relation as

$$\beta_2=\frac{d^2k}{d\omega^2}=\frac{1}{c}\frac{dn_g}{d\omega} \tag{3}$$

The delay-bandwidth product (DBP) is considered as an essential factor for slow light property. The NDBP, which is more useful and convenient, is given by

$$NDBP=n_g\times\frac{\Delta\lambda}{\lambda_c} \tag{4}$$

here, $\Delta\lambda$ is the bandwidth, λ_c is the central wavelength (subscript c represents central).

In the band diagram, there are two modes including one even mode and one odd mode in the PBG as shown in Fig. 2. Both of them are lying below the light line, which means that they are lossless in the vertical direction (perpendicular to the calculating plane) [28]. To confine light in the center core effectively, the even mode is chosen as the main propagation mode for its flat band at

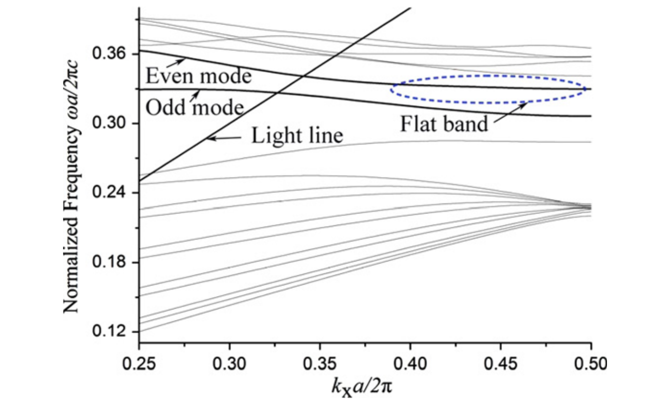

Fig. 2. Calculated dispersion curve of a RSPhCW, where $r=0.34a$. Thick line represents the even mode and the odd mode of the RSPhCW. The dashed circle indicates the flat band on the even mode. Here, $w=0.28a$, $y_1=0.01a$, $y_2=0a$.

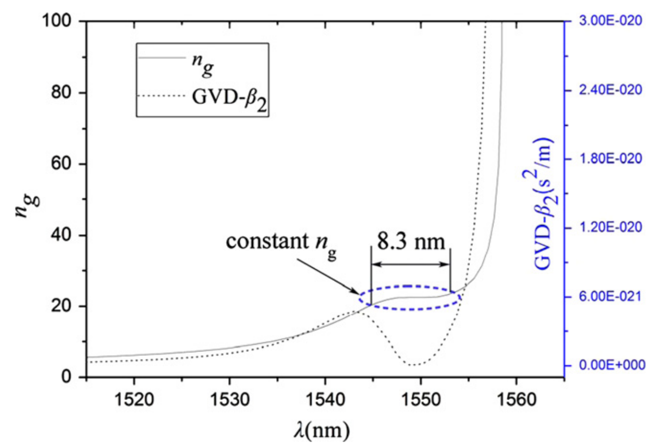

Fig. 3. Group index n_g and the GVD value β_2 as the function of wavelength λ for the even mode in Fig. 2. The dashed circle indicates the constant n_g area.

large wave vectors, shown as the dashed circle in Fig. 2. The corresponding group index curve is shown in Fig. 3. It can be seen that n_g varies rapidly with the wavelength in the large wavelength region and the corresponding GVD value β_2 is very high. Fortunately, there is a constant group index $n_g=23$ (dashed circle in Fig. 3) appearing in the group index curve and the corresponding GVD value β_2 is under $9.19e^{-21}$ s^2/m, which is an allowable value for a typical application of PhCW with a lattice constant $a=520$ nm for a central wavelength of 1550 nm [25,29]. The bandwidth of this constant n_g is 8.3 nm from 1545.4 nm to 1553.7 nm (consider n_g within $\pm 10\%$). The corresponding NDBP=0.12. This constant n_g and the low GVD value β_2 are very meaningful to prevent the high speed signal from severe distortion in transmission.

The even mode in Fig. 2 can be divided into index-guided region and gap-guided region, which would help to understand the generating mechanism of the guided mode in RSPhCW [30]. When the wave vector is small, the guided mode is well bound to the waveguide core and the mode profile is similar to that of the fundamental mode in a ridge waveguide. The slope of the dispersion curve is large, which indicates a small n_g. Thus, this region is referred to be index-guided region and the mode in this region is called index-guided mode. When the wave vector is large, the guided mode penetrates into the ring-shape-hole PhC lattice, and the slope of the dispersion curve is decreased rapidly, which indicates a large n_g. Hence, this region is referred to be gap-guided region, and the guided mode is gap-guided mode. On the whole, the

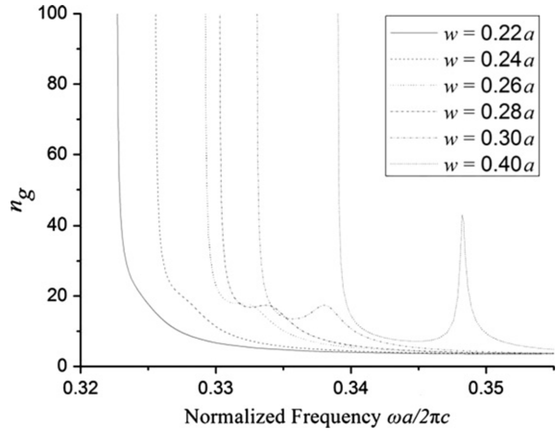

Fig. 4. Group index curves for different shifts of the slot width $w=0.22a$, $0.24a$, $0.26a$, $0.28a$, $0.30a$, $0.32a$, $0.40a$, respectively.

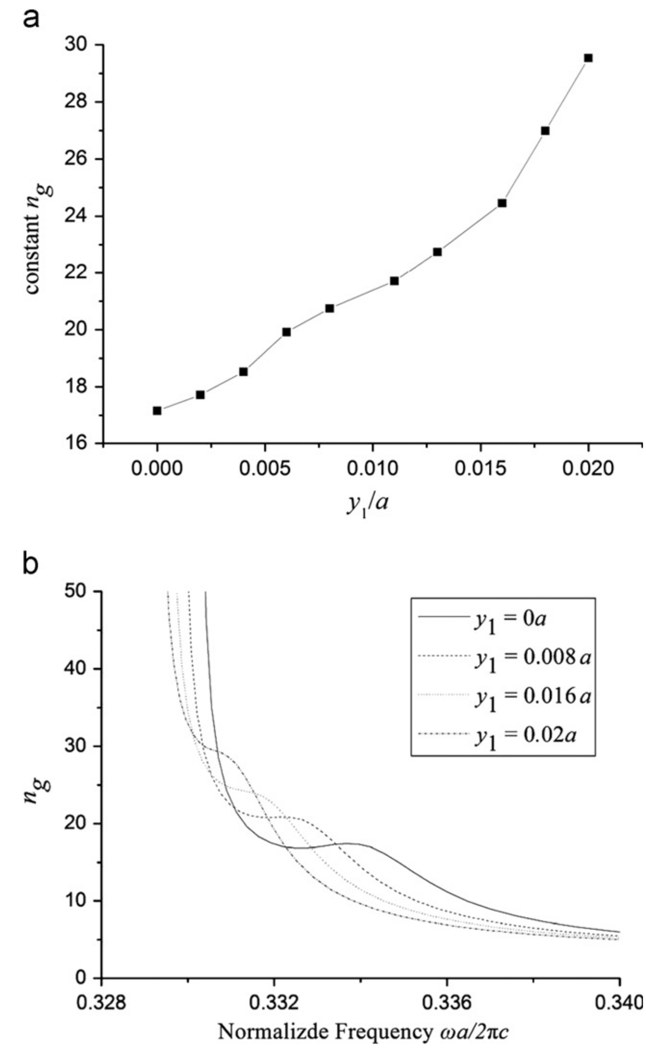

Fig. 5. (a). The group index n_g as a function of the position of y_1. (b). Group index curves for different shifts of the first row from $y_1=0a$ to $y_1=0.02a$ with $w=0.28a$, $y_2=0a$.

even PBG mode is an interaction between the index-guided mode and the gap-guided mode.

Fig. 4 shows the group index curves for different shifts of the slot width $w=0.22a$, $0.24a$, $0.26a$, $0.28a$, $0.30a$, $0.32a$, $0.40a$, respectively. It can be seen that a step-like behavior is found and a constant n_g is occurred when $w=0.26a$ and $0.28a$, which inhibits an ideal low GVD value β_2 and a high constant n_g. When w is larger than $0.28a$, the step shape of the group index curve turns into a pulse peak gradually, which means that the constant n_g is vanished and the GVD value β_2 is increased. So $w=0.26a$ and $w=0.28a$ are both appropriate. $w=0.28a$ is chosen in the following calculation. From Fig. 4, it is also found that the constant n_g is decreased from 18 to 17 as w is changed from $0.26a$ to $0.28a$, which can be used to fine-tune the constant n_g in slotted PhCW designing. The blue shift of the group index curve, when w is increased, will be discussed later in the following text.

In the calculation, it is found that the band frequency curve and the group index curve are both very sensitive to the RSPhCW configuration and structural parameters. Considering available fabrication technique, two parameters y_1 and y_2 are chosen to optimize the slow light property of the RSPhCW. Here, y_1 represents the distance of the ring-shape-holes, in the row adjacent to the central slot, away from the original position (subscript 1 represents the first row); y_2 represents the distance of the ring-shape-holes, in the second row adjacent to the central slot, away from the original position (subscript 2 represents the second row) as shown in Fig. 1.

First, when y_2 is kept constant, the constant n_g is increased as y_1 is increased as shown in Fig. 5(a). The corresponding group index curves for different y_1 are shown in Fig. 5(b). It can be seen that the constant n_g is increased from 17 to 30 when y_1 is increased from $0a$ to $0.02a$. At the same time, the group index curve is red shifted, which means that the lower cutoff frequency of the guided mode in the PBG is decreased. The numerical results show that for constant group indices of 17, 21, 24 and 30, the NDBPs are 0.15, 0.14, 0.11 and 0.09.

Using the coupled-mode theory [31], these phenomena can be explained. As we know, the coupling between forward and backward propagating modes originates PBG in a 1D Bragg grating, and the bandwidth of the gap depends on the coupling strength. Likewise, the coupling between the contra-directional modes produces the PBG in the RSPhCW. Based on the electromagnetic variational theorem [28], it is also known that the low frequency modes are restricted to the high-ε region, and the high frequency modes are restricted to the low-ε region. The decrease of w or the increase of y_1 causes an increase of the effective index of refraction in the waveguide core. As a result, the guided mode of the waveguide moves from the high frequency area to the low one. At the same time, the coupling strength between the defect mode and the low frequency mode is strengthened, and the one between the defect mode and the high frequency mode is weakened. Therefore, the bandwidth of the guided mode at high frequency area, namely, the gap-index region in our model, is decreased. The slope of the dispersion curve is decreased, and v_g is decreased too. In the end, n_g is increased and the even PBG mode is red shifted, when y_1 is increased or w is decreased.

Second, when y_1 is kept constant, the constant n_g is decreased as y_2 is increased as shown in Fig. 6(a). The corresponding group index curves for different y_2 are shown in Fig. 6(b). It can be seen that the constant n_g is decreased from 25 to 16 when y_2 is increased from $-0.04a$ to $0.04a$. At the same time, the group index curve is red shifted, which means that the lower cutoff frequency of the guided mode in the PBG is decreased. The numerical results show that for constant group indices of 25, 24, 23, 19 and 16, the NDBPs are 0.12, 0.12, 0.12, 0.14 and 0.14.

To explain the phenomena above, the slab between the first and second row of ring-shape-holes adjacent to the slot should be considered as a giant cavity [8]. The increase of y_2 enlarges this giant cavity. According to the coupled-mode theory, the coupling between the cavity mode and the slot mode is strengthened.

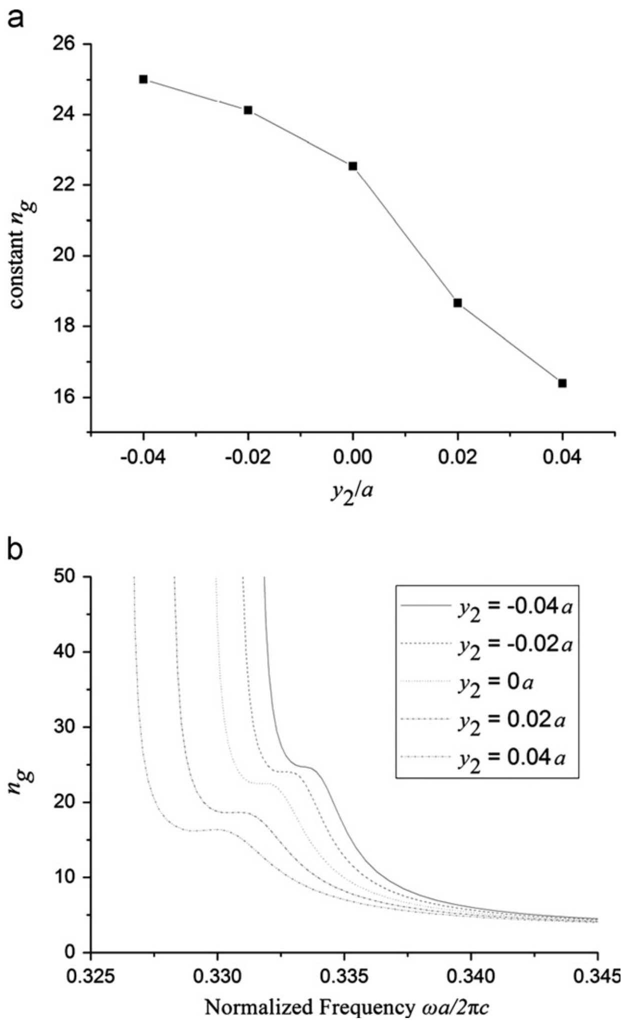

Fig. 6. (a). The group index n_g as a function of the position of y_2. (b). Group index curves for different shifts of the second row from $y_2=-0.04a$ to $y_2=0.04a$ with $w=0.28a$, $y_1=0.01a$.

The bandwidth is enlarged and the slope of the guided band is enlarged too. Then, v_g is increased and n_g is decreased. At the same time, the increase of y_2 causes an increase of the effective index of refraction in the waveguide core. The guided mode of the waveguide moves from the high frequency area to the low one. Therefore, the red shift of the group index curve is occurred. Eventually, n_g is decreased and the even PBG mode is red shifted, when y_2 is increased.

Based on the discussion above, the optimized RSPhCW with high constant n_g and low GVD value β_2 is available by tuning y_1 and y_2 together. It must be mentioned that if y_1 and y_2 are too large, the constant n_g would disappear and the pulse peak shape would emerge as in Fig. 4. Our procedure is as follows: first, y_1 is tuned separately. The constant group indices, the GVD values, and the NDBPs are calculated to estimate y_1 for appropriate values. Then y_2 is tuned finely, and the constant n_g is further enlarged.

Three examples for optimized RSPhCW are given. For $y_1=0.004a$, $y_2=0.03a$, the constant $n_g=15$ is from 1541.7 nm to 1559.0 nm with the bandwidth $\Delta\lambda=17.3$ nm. The NDBP$=0.17$, as shown in Fig. 7. For $y_1=0.02a$, $y_2=-0.03a$, the constant $n_g=34$ is from 1549.1 nm to 1554.0 nm with the bandwidth $\Delta\lambda=4.9$ nm. The NDBP$=0.11$, as shown in Fig. 8. For $y_1=0.031a$, $y_2=-0.042a$, the constant $n_g=67$ is from 1550.3 nm to 1552.1 nm with the bandwidth $\Delta\lambda=1.8$ nm. The NDBP$=0.08$, as shown in Fig. 9.

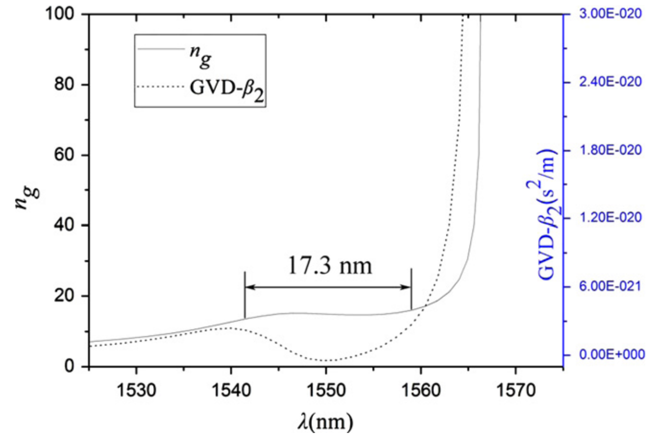

Fig. 7. Group index n_g and the GVD value β_2 plotted as the function of wavelength λ for the case with $w=0.28a$, $y_1=0a$, $y_2=-0.01a$.

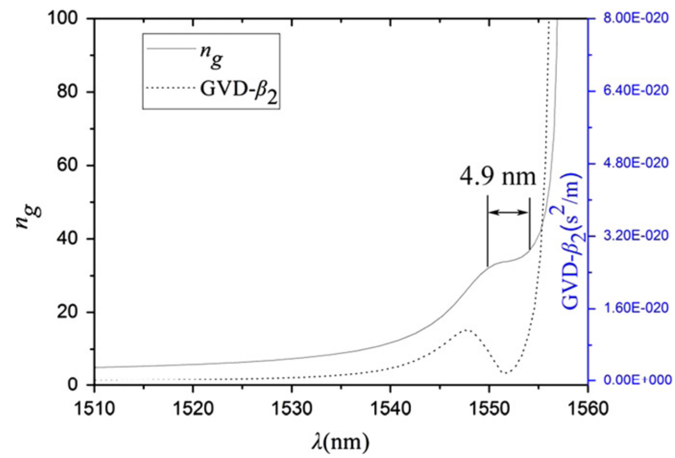

Fig. 8. Group index n_g and the GVD value β_2 plotted as the function of wavelength λ for the case with $w=0.28a$, $y_1=0.02a$, $y_2=0a$.

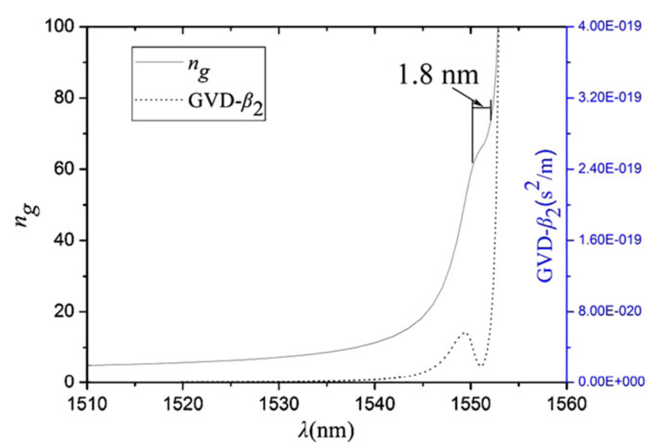

Fig. 9. Group index n_g and the GVD value β_2 plotted as the function of wavelength λ for the case with $w=0.28a$, $y_1=0.03a$, $y_2=-0.04a$.

3. Conclusion

In summary, a new type of RSPhCW is constructed and simulated. The effects of the parameters, i.e., the width of the central slot w, the positions of the first and second rows with ring-shape-holes adjacent to the central slot y_1 and y_2, on the slow light property are analyzed and discussed. It is numerically demonstrated that, the constant n_g is increased when w and y_2 are decreased or y_1 is increased. Meanwhile, the group index curve is red-shifted when w is decreased or y_1 and y_2 are increased. Optimized examples are realized by tuning these parameters. RSPhCWs with the constant indices of 15, 34, 67 over 17.3 nm, 4.9 nm and 1.8 nm bandwidth, repectively, are demonstrated. The corresponding NDBPs are 0.17, 0.11 and 0.08. The results are of reference value for designing PhCW with slow light property.

Acknowledgements

This work is supported by the MOST of China (2007CB936204) and the NSFC (60971002, 61076057 and 61171023).

References

[1] T. Baba, Nature Photonics 2 (2008) 465.
[2] T.F. Krauss, Journal of Physics D: Applied Physics 40 (2007) 2666.
[3] C. Koos, P. Vorreau, T. Vallaitis, P. Dumon, W. Bogaerts, R. Baets, B. Esembeson, I. Biaggio, T. Michinobu, F. Diederich, W. Freude, J. Leuthold, Nature Photonics 3 (2009) 216.
[4] B. Corcoran, C. Monat, C. Grillet, D.J. Moss, B.J. Eggleton, T.P. White, L. O'Faolain, T.F. Krauss, Nature Photonics 3 (2009) 206.
[5] Y.A. Vlasov, M. O'Boyle, H.F. Hamann, S.J. McNab, Nature 438 (2005) 65.
[6] A.Y. Petrova, M. Eich, Applied Physics Letters 85 (2004) 4866.
[7] D.M. Beggs, L. O'Faolain, T.F. Krauss, Physica E 41 (2009) 1115.
[8] K.T. Zhu, T.S. Deng, Y. Sun, Q.F. Zhang, J.L. Wu, Optics Communication 285 (2012) 2611.
[9] J. Hou, H.M. Wu, D.S. Citrin, W.Q. Mo, D.S. Gao, Z.P. Zhou, Optics Express 18 (2010) 10567.
[10] L.Y. Liu, D.Q. Yang, H.P. Tian, Y.F. Ji, Optics Communication 285 (2012) 171.
[11] D.B. Wang, J. Zhang, L.H. Yuan, J.L. Lei, S. Chen, J.W. Han, S.L. Hou, Optics Communication 284 (2011) 5829.
[12] J. Wu, Y.P. Li, C. Peng, Z.Y. Wang, Optics Communication 283 (2010) 2815.
[13] C. Monat, B. Corcoran, M. Ebnali-Heidari, C. Grillet, B.J. Eggleton, T.P. White, L. O'Faolain, T.F. Krauss, Optics Express 17 (2009) 2944.
[14] Y. Hamachi, S. Kubo, T. Baba, Optics Letters 34 (2009) 1072.
[15] J.T. Li, T.P. White, L. O'Faolain, A. Gomez-Iglesias, T.F. Krauss, Optics Express 16 (2008) 6227.
[16] V.R. Almeida, Q.F. Xu, C.A. Barrios, M. Lipson, Optics Letters 29 (2004) 1209.
[17] A. Di Falco, L. O'Faolain, T.F. Krauss, Photonics and Nanostructures - Fundamentals and Applications 6 (2008) 38.
[18] L.Y. Wang, K. Hoshino, X.J. Zhang, Optics Letters 36 (2011) 1917.
[19] K.Y. Cui, Q. Zhao, X. Feng, Y.D. Huang, Y.Z. Li, D. Wang, W. Zhang, Thermo-optic Switch Based on Transmission-dip Shifting in a Double-slot Photonic Crystal Waveguide 100 (2012) 201102.
[20] A. Di Falco, L. O'Faolain, T.F. Krauss, Applied Physics Letters 92 (2008) 083501.
[21] R.J.P. Engelen, Y. Sugimoto, Y. Watanabe, J.P. Korterik, N. Ikeda, N.F. van Hulst, K. Asakawa, L. Kuipers, Optics Express 14 (2006) 1658.
[22] A. Säynätjoki, K. Vynck, M. Mulot, D. Cassagne, J. Ahopelto, H. Lipsanen, Photonics and Nanostructures: Fundamentals and Applications 6 (2008) 127.
[23] J. Hou, D.S. Gao, H.M. Wu, R. Hao, Z.P. Zhou, IEEE Photonics Technology Letters 21 (2009) 1571.
[24] Y. Zhai, H.P. Tian, Y.F. Ji, Journal of Lightwave Technology 29 (2011) 3083.
[25] M. Mulot, A. Säynätjoki, S. Arpiainen, H. Lipsanen, J. Ahopelto, Journal of Optics A: Pure and Applied Optics 9 (2007) S415.
[26] A. Säynätjoki, M. Mulot, J. Ahopelto, H. Lipsanen, Optics Express 15 (2007) 8323.
[27] D.S. Gao, Z.P. Zhou, Applied Physics Letters 88 (2006) 163105.
[28] J.D. Joannopoulos, S.G. Johnson, J.N. Winn, R.D. Meade, Photonic Crystals: Molding the Flow of Light, second ed., Princeton University Press, Princeton, 2008.
[29] J. Ma, C. Jiang, IEEE Photonics Technology Letters 20 (2008) 1237.
[30] L.H. Frandsen, A.V. Lavrinenko, J. Fage-Pedersen, P.I. Borel, Optics Express 14 (2006) 9444.
[31] O. Khayam, H. Benisty, Optics Express 17 (2009) 14634.